Proc. Natl. Acad. Sci. USA
Vol. 90, pp. 7711–7715, August 1993
Immunology

Three-dimensional structure of a heteroclitic antigen–antibody cross-reaction complex

(crystal structure/heteroclitic antibody/lysozyme)

VÉRONIQUE CHITARRA, PEDRO M. ALZARI, GRAHAM A. BENTLEY*, T. NARAYANA BHAT, JEAN-LUC EISELÉ, ANNE HOUDUSSE, JULIEN LESCAR, HÉLÈNE SOUCHON, AND ROBERTO J. POLJAK†

Unité d'Immunologie Structurale (Centre National de la Recherche Scientifique, Unité de Recherches Associée URA 359), Institut Pasteur, 25 rue du Dr. Roux, 75724 Paris Cedex 15, France

Communicated by César Milstein, April 29, 1993

ABSTRACT **Although antibodies are highly specific, cross-reactions are frequently observed. To understand the molecular basis of this phenomenon, we studied the anti-hen egg lysozyme (HEL) monoclonal antibody (mAb) D11.15, which cross-reacts with several avian lysozymes, in some cases with a higher affinity (heteroclitic binding) than for HEL. We have determined the crystal structure of the Fv fragment of D11.15 complexed with pheasant egg lysozyme (PHL). In addition, we have determined the structure of PHL, Guinea fowl egg lysozyme, and Japanese quail egg lysozyme. Differences in the affinity of D11.15 for the lysozymes appear to result from sequence substitutions in these antigens at the interface with the antibody. More generally, cross-reactivity is seen to require a stereochemically permissive environment for the variant antigen residues at the antibody–antigen interface.**

Cross-reactions between antibodies and differing antigens have been observed since the earliest immunochemical studies. At times, this behavior has been taken to represent an intrinsic property by which antibodies might participate in degenerate binding and thus amplify the functional diversity of the immune system without incurring a severe loss of specificity (1). Heteroclitic reactions (2), in which antigens not used in challenging the immune system bind better to the elicited antibodies than does the immunogen itself, are a corollary to cross-reactivity.

To study the fine specificity of the monoclonal antibodies (mAbs) to hen (*Gallus domesticus*) egg-white lysozyme (HEL) obtained in our laboratory, we have used seven different egg-white avian lysozymes for cross-reactivity studies: partridge (*Perdix perdix*) (PEL), California quail (*Lophortyx californica*) (CEL), bobwhite quail (*Colinus virginianus*) (BEL), Japanese quail (*Coturnix coturnix japonica*) (JEL), turkey (*Meleagris gallopavo*) (TEL), pheasant (*Phasianus colchicus*) (PHL), and Guinea fowl (*Numida meleagris*) (GEL). The patterns of observed antibody binding allowed us to classify these mAbs into 10 different classes, 2 of which are very distinct and seemingly contrasting (3). The first is typified by mAb D1.3, which cross-reacts with high affinity with only one of the test lysozymes listed above, namely BEL. The three-dimensional structure of the complex FabD1.3–HEL (4–6) shows that the fine specificity of this mAb arises, in particular, from the sterically confined and chemically specific environment of residue 121 of lysozyme at the antibody–antigen interface; the side chain of Gln (HEL or BEL) may be readily accommodated but not that of His (PEL, CEL, or TEL), Asp (JEL or PHL), or Arg (GEL). A very different pattern of fine specificity is shown by mAb D11.15, which binds strongly to all the test lysozymes. Furthermore, the equilibrium association constants for the reaction of D11.15 show a higher affinity for PHL and GEL compared with HEL, while that for JEL is lower (3). Thus, D11.15 cross-reacts extensively with the different lysozymes and shows a heteroclitic reaction with two of them.

To investigate cross-reactivity and heteroclitic binding at the structural level, we crystallized the heteroclitic complex FabD11.15–PHL (7). Subsequently, we obtained the recombinant, bacterially expressed, FvD11.15 and crystallized it also as a complex with PHL. The crystal structure of the Fv complex with PHL has been determined by x-ray diffraction, as has the crystal structure of three lysozymes—JEL, GEL, and PHL—which are important for the analysis of the cross-reactivity and heteroclitic behavior of mAb D11.15.§ We also report affinity measurements of D11.15 for HEL, PHL, GEL, and JEL obtained by a method alternative to that reported earlier (3).

MATERIALS AND METHODS

Affinity Measurements on D11.15. The affinities of D11.15 for HEL, PHL, GEL, and JEL were measured by using the BIAcore (Pharmacia Biosensor) system, which is based on detection of surface plasmon response from a specially prepared surface onto which the interacting molecules are adsorbed (8). All solutions were prepared from PBS (phosphate-buffered saline; 100 mM sodium phosphate/150 mM NaCl) at pH 7.4 and the protocol described elsewhere (8) was followed. Rabbit anti-mouse Fc immunoglobulin, bound to the sensor clip of the BIAcore system, was used to capture mAb D11.15. Each lysozyme was then passed in turn over the sensor clip to measure the association rate. Dissociation rates were determined from the rate of loss of lysozyme when its flow over the clip was replaced by a flow of buffer.

Crystallization and Structure Determination. The Fv fragment of D11.15 was cloned and expressed as previously described (10). The FvD11.15–PHL complex was crystallized in hanging drops by vapor diffusion against 17.5% (wt/vol) PEG 8000/0.1 M potassium phosphate, pH 8.5. The space group is $P6_5$, with unit cell dimensions a = 57.8 Å and c = 281.2 Å, and one molecule of the complex in the

The publication costs of this article were defrayed in part by page charge payment. This article must therefore be hereby marked "*advertisement*" in accordance with 18 U.S.C. §1734 solely to indicate this fact.

Abbreviations: mAb, monoclonal antibody; HEL, hen egg lysozyme; PHL, pheasant egg lysozyme; JEL, Japanese quail egg lysozyme; BEL, bobwhite quail egg lysozyme; CEL, California quail egg lysozyme; GEL, Guinea fowl egg lysozyme; PEL, partridge egg lysozyme; TEL, turkey egg lysozyme; H, heavy; L, light; V, variable; CDR, complementarity-determining region.

*To whom reprint requests should be addressed.
†Present address: Center of Advanced Research in Biotechnology, 9600 Gudelsky Drive, Rockville, MD 20850.

§The atomic coordinates have been deposited in the Protein Data Bank, Chemistry Department, Brookhaven National Laboratory, Upton, NY 11973 (references 1JHL for FvD11.15–PHL, 1GHL for PHL, 1HHL for GEL, and 1IHL for JEL).

asymmetric unit. X-ray diffraction data were measured on a Siemens-Xentronic area detector using monochromated Cu-Kα x-radiation from a rotating anode generator. The crystal-to-detector distance was 280 mm and three detector angle settings (11°, 18°, and 27°) were used to collect diffraction data to 2.4-Å resolution. The data, measured from four crystals and nine separate crystal orientations, were processed by using the program XDS (11); 94,553 observations were merged and scaled, giving 19,835 independent reflections (95% complete) with a R_{sym} of 13.9%. The structure was determined by molecular replacement using the variable dimer of FabE225 (12) and HEL (13) separately as search models for the two components of the complex. The space group was shown to be $P6_5$ and not its enantiomorph, $P6_1$. The independent treatment of the two search components assembled them into a complex in which the complementarity-determining regions (CDRs) of the Fv made contacts with lysozyme. Intermolecular contacts of the model complex gave a feasible network of interactions in the crystal lattice with no steric clashes between neighboring molecules, giving us further confidence that the correct solution had been found. Finally, this result proved to be consistent with the anticipated epitope of lysozyme (3).

The structure was refined by using X-PLOR (14), giving an R factor of 21.4% [based on 16,483 reflections between the resolution limits of 7.0 and 2.4 Å for which $F > 3\sigma(F)$] and an rms deviation from ideal bond lengths of 0.020 Å in the final model. During the course of refinement, 206 solvent molecules were added to the model. About 150 of these were used to model an extensive discontinuous density confined to a rather well-defined volume about 20 × 25 × 25 Å^3. There was no significant electron density in the solvent region outside of this volume, except close to the surface of the protein. Although further searches by molecular replacement failed to produce evidence for additional structure, this residual density did not have the typical aspect of solvent and might thus indicate the presence of a further molecule (for example, lysozyme) in a low occupancy and/or disordered state. The σ_a plot (15) was consistent with this interpretation, since it indicated that one molecule of complex accounted for essentially all of the well-ordered diffracting material in the unit cell. This plot, in addition, showed the rms error in the atomic coordinates to be 0.3 Å.

To test the validity of our modeling of the disordered region, we adopted a procedure similar to that described by Brünger (16). Two separate runs of refinement using X-PLOR were performed, using a set of structure amplitudes from which 10% of the data had been removed at random; in the first run the solvent molecules modeling the disordered density were included in the calculation, while in the second they were removed. With all atoms from the protein and solvent included, the R factor was 21.6% for the 90% of the data retained for the refinement and 33.6% for the 10% removed. When solvent modeling the disordered density was excluded from the refinement, the R factor for the rejected 10% of the data rose to 37.5%. The larger increase in R factor for the 10% of removed data (which should not be biased by the refined atomic parameters) upon excluding the solvent suggests that additional structure over and above the complex itself is required to account for the diffraction data and that this is achieved, in part at least, by the additional atoms used to model the disordered density.

Structures of Lysozymes. The crystal structures of the lysozymes PHL, GEL, and JEL were also determined to provide a firm structural base for describing the cross-reactivity of mAb D11.15. These were all solved by molecular replacement and refined at high resolution; crystallographic details of the data analysis and refinement are given in Table 1. Fuller descriptions of these analyses will be published elsewhere.

RESULTS AND DISCUSSION

Affinities of D11.15 for HEL, PHL, GEL, and JEL. Association and dissociation rates were measured as described (8) and the affinity constants were calculated directly from these rates; the results are shown in Table 2. These measurements are in agreement with the relative association constants determined earlier (3) by binding inhibition studies. The association rate constants of HEL, PHL, GEL, and JEL are high and almost equal to each other. Such similarity might suggest the rate-determining step in complex formation to be the approach of the antigen in a productive orientation; the identical dimensions of the different lysozyme species should lead to equivalent effects from both diffusion and orientation factors on the kinetics of this particular step of the reaction. Conformational adaptation of the antigen and antibody upon contact could be expected to follow on a shorter time scale (17) and thus should not influence the forward kinetics. Dissociation rate constants, on the other hand, should reflect more directly any differences in the interactions between the antibody and the different antigens. The observed rates of dissociation show a dispersion of values; both PHL and GEL dissociate from D11.15 about 1/4 to 1/5 as rapidly as HEL while JEL, by comparison, dissociates about 3 times more rapidly (see Table 2). The affinity (equilibrium) constants of D11.15 for the four lysozymes are higher than those obtained between D1.3 and HEL, either by ELISA (3) or by the BIAcore method, and may be due, in part, to the presence of two well-defined salt bridges formed between D11.15 and lysozyme (see Table 3).

Description of the FvD11.15–PHL Structure. The Fv fragment of D11.15 interacts with PHL through residues belonging to all three CDR loops of the heavy chain variable domain (V_H) but only the third CDR of the light chain variable domain (V_L); no direct contacts involving framework residues are present. The epitope recognized by D11.15 is discontinuous and, broadly speaking, includes the regions 21–23, 103–106,

Table 1. Crystallographic data for lysozyme structures

Data	PHL	GEL	JEL
Space group	$P4_32_12$	$P6_12_12$	$C2$
Unit cell	$a = b = 98.9$ Å, $c = 69.3$ Å	$a = b = 89.2$ Å, $c = 61.7$ Å	$a = 103.9$ Å, $b = 38.7$ Å, $c = 34.0$ Å, $\beta = 100.6°$
Molecules in asymmetric unit	2	1	1
Total reflections/ unique reflections	91,751/19,434	80,452/11,788	78,738/26,121
R_{sym}	8.3%	11.4%	8.4%
Max. resolution	2.1 Å	1.9 Å	1.4 Å
R factor/no. of refs.	17.8%/16,122	16.7%/8,854	16.5%/19,119
σ(bond)/σ(angle)	0.010 Å/2.5°	0.010 Å/2.5°	0.016 Å/1.5°
Water molecules	140	87	151

Table 2. Rate and affinity constants for complex formation between mAb D11.15 and HEL, PHL, GEL, and JEL

Lysozyme	k_{ass}, $M^{-1}s^{-1}$ $\times 10^{-6}$	k_{diss}, s^{-1} $\times 10^{4}$	K_a, M^{-1} $\times 10^{-9}$
HEL	4.4	11	4.0
PHL	3.3	2.2	15
GEL	4.3	2.1	20
JEL	3.9	27	1.5

and 112–119 of lysozyme. A total of 12 antibody residues interact directly with 10 lysozyme residues. Interatomic contacts across the antibody–antigen interface, which include five hydrogen bonds and two salt bridges, are listed in Table 3. Criteria for defining interatomic contacts are given in the legend of the table; these correspond to definitions used by other workers (18). A general view in stereo of the region of interaction between antibody and antigen is presented in Fig. 1; the residues involved in direct contact across the antibody–antigen interface are labeled, with hydrogen bonds and salt bridges indicated as broken lines. The salt bridges are made to antigen residues which are invariant within the panel of seven lysozymes used for cross-reaction studies, namely, Arg-112 [to Asp-55 (V_H)] and Lys-116 [to Asp-99 (V_H)]. The total loss of solvent-accessible surface area upon formation of the Fv complex, calculated with the algorithm of Kabsch and Sander (19) using a solvent probe radius of 1.4 Å, is 648 $Å^2$ for the antibody fragment and 681 $Å^2$ for the PHL moiety.

Description of the Lysozyme Structures. The main chain atoms of PHL in the Fv complex, PHL in the free form (the two independent molecules of the asymmetric unit), GEL, and JEL were optimally superimposed upon those of uncomplexed HEL in the tetragonal crystal form (13); this showed the rms deviations with respect to HEL to be 0.59, 0.45, 0.55, 0.85, and 1.02 Å, respectively. The largest differences occur in the regions 70–73 and 100–104 (the latter was not used in the calculated rms differences above), which can amount to as much as 2 Å or more. These regions correspond to flexible loop structures at the surface of the molecule whose conformation can be easily influenced by the local environment in the crystal lattice. Changes in lysozyme structure due to binding by antibody cannot be distinguished from those found in the different uncomplexed forms, where different crystalline environments are probably the main cause of structural variation. Thus, even though some of the larger differences seen between free and antibody-bound PHL occur in the loop 100–104, which contributes to the epitope, they are similar in magnitude to those found between the different uncomplexed lysozyme structures.

Table 3. Interatomic contacts in the complex FvD11.15–PHL

D11.15 CDR	D11.15 Residue	PHL residue	No. of contacts	Polar contacts
L3	Asn-92	Thr-118	2	
		Asp-119	1	
	Glu-93	Gly-117	5	
	Tyr-94	Lys-116	2	
		Gly-117	12	1 H bond
	Trp-96	Gly-117	1	
H1	Ser-31	Asn-103	2	1 H bond
	Trp-33	Asn-106	4	1 H bond
		Arg-112	1	
		Lys-116	6	
H2	Tyr-52	Asn-106	3	
		Arg-112	2	
	Asp-55	Arg-112	2	1 salt bridge
	Tyr-57	Lys-113	5	
H3	Asp-99	Lys-116	3	1 salt bridge
	Asn-101	Tyr-23	5	1 H bond
	Tyr-102	Arg-21	3	1 H bond
		Tyr-23	7	

Upper interatomic distances for defining interatomic contact between antibody and antigen are as follows: C–C, 4.1 Å; C–N, 3.8 Å; C–O, 3.7 Å; O–O, 3.3 Å; O–N, 3.4 Å; N–N, 3.4 Å. L3 is the third CDR of V_L; H1, H2, and H3 are the first, second, and third CDRs of V_H.

The structure of JEL reveals an important change in conformation for the loop bounded by residues 100 and 104. The difference begins at residue 100, where the polypeptide chain takes an alternative course, differing from the HEL structure by up to 7.5 Å in the main-chain atom positions before returning back to the consensus lysozyme structure at residue 105. This loop contains two amino acid differences with respect to HEL, namely 102 (Gly in HEL, Val in JEL) and 103 (Asn in HEL, His in JEL). As we shall discuss below, this structural difference is sufficient to account for the reduced affinity of D11.15 for JEL, since this region forms part of the epitope. The different conformation in JEL no doubt arises from the amino acid substitution at position 102, where the ϕ–ψ angles in HEL are favorable for Gly only.

Specificity of mAb D11.15. The structure of the antibody–antigen complex shows that two differences in amino acid sequence between HEL and PHL may be implicated in the heteroclitic behavior of D11.15. These are at position 113 (Asn in HEL, Lys in PHL) and position 121 (Gln in HEL, Asn in PHL). In the crystal structure of the complex, Lys-113 of PHL makes nonpolar contacts with residue Tyr-57 (V_H) (Table 3). It is curious that even though the amino group of Lys-113 is 4.5 Å from the carboxyl group of Asp-55 (V_H) in the crystal structure, we find no steric constraint against a closer approach of this group to form a salt bridge. Electron density for the side chain of Lys-113 (PHL) was still present in a difference Fourier map after removing its atoms from the coordinate file and performing a round of refinement with the program X-PLOR, essentially confirming our interpretation of the structure for this residue. A view of the complex and electron density in this region is given in Fig. 2. Modeling the HEL complex by replacement of Lys by Asn at lysozyme position 113 in FvD11.15–PHL shows that this amino acid residue might also make nonpolar contacts with the antibody. Thus, while it is not immediately clear from the structure how this difference in antigen sequence might influence binding, we would not like to exclude at this stage a possible explanation arising from electrostatic effects. The heterologous antigen GEL has, like PHL, a Lys residue at position 113 and should interact in a similar way with D11.15.

Although Asn-121 (PHL) does not make direct intermolecular contact with D11.15 in the crystal structure, it approaches Ser-30 (V_L) to within a distance of 3.9 Å. Modeling the HEL complex by replacing Asn by Gln at position 121 of lysozyme in the FvD11.15–PHL complex (see Fig. 1) shows that Gln-121 of HEL can make a closer approach to the antibody, conceivably forming a hydrogen bond with Ser-30 (V_L). Furthermore, the longer side chain Arg-121 of GEL may reach even further to the antibody; modeling this amino acid change in the crystal structure of the complex (see Fig. 1) shows that Arg-121 (GEL) could potentially form hydrogen bonds to both Ser-28 and Ser-30 of V_L. Be this as it may, there is no measurable difference in binding affinity between GEL and PHL.

The crystal structure of JEL would account for the lower affinity of D11.15. JEL residues 102 and 103 sterically clash with the third CDR of V_H, and binding to D11.15 would require a conformational change upon formation of the complex. Given the lower observed affinity of D11.15 for JEL, we would conclude that this conformation is energetically less favorable. One additional lysozyme residue involved in direct contacts with D11.15 which differs for JEL is at position 21; here, however, the replacement of Gln by Arg is of little or

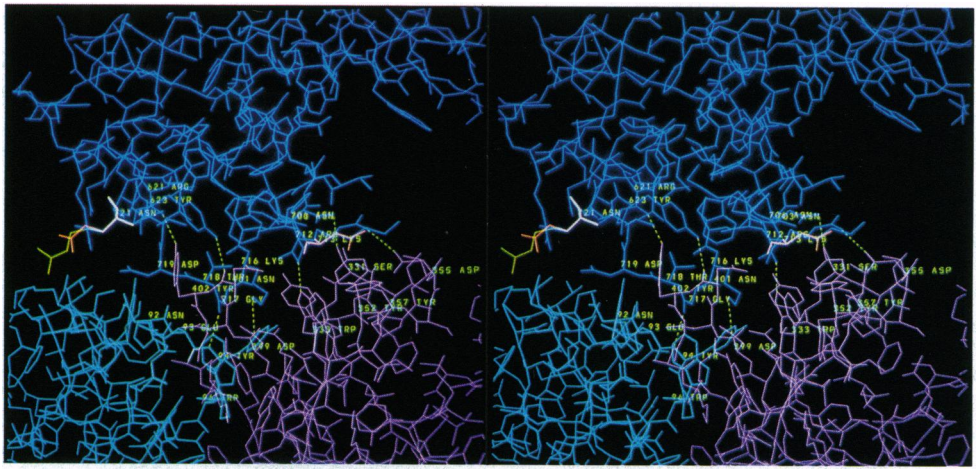

FIG. 1. Stereoview of the antibody–antigen interface of the complex FvD11.15–PHL. The domain V_L is in light blue, V_H in violet, and PHL in dark blue. All residues making direct contacts across the interface, together with PHL residue 121 (721 in the figure), are labeled. In this figure, V_L residues are numbered 1–106, V_H residues are numbered 301–416 (corresponding to 1–116 in Table 3 and text), and PHL residues are numbered 601–729 (corresponding to 1–129 in Table 3 and text). Variant lysozyme residues modeled in the region of the interface, 113 (713 in the figure) and 121 (721 in the figure) are shown: HEL in orange and GEL in yellow. Hydrogen bonds and salt bridges described in Table 3 are shown as broken lines.

no consequence, since contacts are made to the main-chain atoms only.

Since the affinity of mAb D11.15 for PHL and GEL is 4 to 5 times higher than for HEL (Table 2), the standard free energy change for complex formation is 0.8–0.9 kcal/mol in favor of these two antigens (1 kcal = 4.18 kJ). Likewise, the 3-fold reduction in affinity for JEL in comparison to HEL corresponds to a free energy difference of 0.6 kcal/mol. As discussed above, it is difficult to assess the overall effect on the affinity of D11.15 for the different species of lysozyme in simple structural terms from the sum of subtle changes seen in different regions of the antibody–antigen interface. Theoretical estimation of the free energy of antibody–antigen binding requires accurate account of many factors, both enthalpic and entropic, in complex formation. The free energy differences for D11.15 binding to the different lysozymes, based on the kinetic measurements described, correspond to about the level of precision expected from current theoretical calculations (20) and thus limit for the present our conclusions based on simple correlations between the structures and the differences in affinity of D11.15 for the variant lysozymes.

Cross-reactivity and Specificity of Antibodies. Residues belonging to the epitope recognized by D11.15 and which vary in sequence within our panel of cross-reacting lysozymes are all located at the periphery of the antibody–antigen interface (see Fig. 1). This may explain the cross-reactive behavior of this antibody, since partial exposure to the solvent could reduce some of the stereochemical constraints on the packing of these side chains upon complex formation and consequently facilitate binding to the different lysozymes. Conversely, sequence changes in the epitope that are more buried from the solvent may be more difficult to accommodate, particularly if they occupy a close-fitting hapten-like pocket as seen with Gln-121 of HEL in association with D1.3. Comparison of the two complexes, D1.3–HEL and D11.15–PHL, therefore provides a conceptual model to understand the apparently opposing phenomena of high specificity (D1.3) and broader cross-reactivity (D11.15) with different antigens. Both D1.3 and D11.15 are high-affinity antibodies obtained during a secondary immune response to the same immunogen, from the same individual mouse. There is, in fact, partial overlap of the epitopes recognized by D1.3 and D11.15; lysozyme residues Gly-117, Thr-118, and Asp-119 make direct contacts with both antibodies. The amino acid replacement in lysozyme that prevents most species from binding to mAb D1.3 occurs at position 121. This residue is placed centrally within the

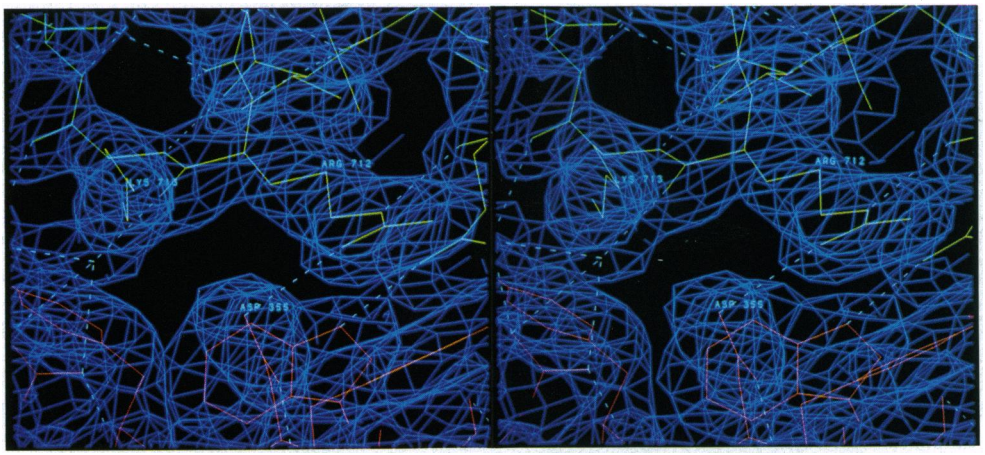

FIG. 2. Stereoview of the structure and electron density in the region of lysozyme residue Lys-113. D11.15 is in red and PHL is in yellow. Hydrogen bonds are shown as broken lines. Lysozyme residues Arg-112 and Lys-113 are labeled ARG 712 and LYS 713, respectively, and Asp-55 (V_H) is labeled ASP 355.

antigen–D1.3 interface in an aromatic pocket between the V_H and V_L domains (6). The close fit in this central location of the interface does not allow for amino acid side chains other than Gln. In addition, position 121 is the most widely varying in amino acid sequence of the test lysozymes used in this study. By contrast, mAb D11.15 has a broad specificity because it binds a "public" epitope, largely shared by different avian lysozymes (sequence replacements in PHL and GEL occur at the edge of the epitope defined by D11.15). Our modeling trials described above show that different amino acids may be sterically accommodated at lysozyme positions 113 and 121 within the D11.15–lysozyme interface.

We note here that immunochemical reactions that can be measured reasonably well by relatively simple techniques (such as binding inhibition), involving less than an order of magnitude difference in affinity, may be difficult to explain by the high-resolution experimental structural analyses we are able to perform. Tulip *et al.* (9) have studied the crystal structures of two mutant neuraminidase–Fab complexes in which the affinity constants are reduced by approximately one order of magnitude. Comparison with the crystal structure of the wild-type neuraminidase–Fab complex has failed to indicate an obvious structural explanation for the reduced affinity. It further illustrates the point that biological specificity and affinity often depend on very subtle structural parameters.

We thank B. Persson of Pharmacia Biosensor (Uppsala, Sweden) for the determination of the affinity constants. This work was supported by grants from the Pasteur Institute and the Centre National de la Recherche Scientifique.

1. Richards, F. F., Konigsberg, W. H., Rosenstein, R. W. & Varga, J. M. (1975) *Science* **187**, 130–137.
2. Mäkelä, O. (1965) *J. Immunol.* **95**, 378–386.
3. Harper, M., Lema, F., Boulot, G. & Poljak, R. J. (1987) *Mol. Immunol.* **24**, 97–108.
4. Amit, A. G., Mariuzza, R. A., Phillips, S. E. V. & Poljak, R. J. (1986) *Science* **233**, 747–753.
5. Bhat, T. N., Bentley, G. A., Fishmann, T. O., Boulot, G. & Poljak, R. J. (1990) *Nature (London)* **347**, 483–485.
6. Fischmann, T. O., Bentley, G. A., Bhat, T. N., Boulot, G., Mariuzza, R. A., Phillips, S. E. V., Tello, D. & Poljak, R. J. (1991) *J. Biol. Chem.* **266**, 12915–12920.
7. Guillon, V., Alzari, P. M. & Poljak, R. J. (1987) *J. Mol. Biol.* **197**, 375–376.
8. Karlsson, R., Michaelsson, A. & Mattsson, L. (1991) *J. Immunol. Methods* **145**, 229–240.
9. Tulip, W. R., Varghese, J. N., Webster, R. G., Laver, W. G. & Colman, P. M. (1992) *J. Mol. Biol.* **227**, 149–159.
10. Eiselé, J. L., Boulot, G., Chitarra, V., Riotott, M. M., Houdouse, A., Bentley, G. A., Bhat, T. N., Spinelli, S. & Poljak, R. J. (1992) *J. Crystallogr. Growth* **122**, 337–343.
11. Kabsch, W. (1988) *J. Appl. Crystallogr.* **21**, 916–924.
12. Bentley, G. A., Boulot, G., Riottot, M. M. & Poljak, R. J. (1990) *Nature (London)* **348**, 254–257.
13. Kundrot, C. E. & Richards, F. M. (1987) *J. Mol. Biol.* **193**, 157–170.
14. Brünger, A., Kuriyan, J. & Karplus, M. (1987) *Science* **235**, 458–460.
15. Read, R. J. (1986) *Acta Crystallogr.* **A42**, 140–149.
16. Brünger, A. (1992) *Nature (London)* **355**, 472–475.
17. Gurd, F. R. N. & Rothgeb, T. M. (1979) *Adv. Prot. Chem.* **33**, 73–165.
18. Tulip, W. R., Varghese, J. N., Webster, R. G., Air, G. M., Laver, W. G. & Colman, P. M. (1989) *Cold Spring Harbor Symp. Quant. Biol.* **54**, 257–263.
19. Kabsch, W. & Sander, C. (1983) *Biopolymers* **22**, 2577–2637.
20. McCammon, J. A. (1991) *Curr. Opin. Struct. Biol.* **1**, 196–200.